Strain dependence of the interface perpendicular magnetic anisotropy in epitaxial Co/Au/Cu(111) films

Akihiro Murayama,* Kyoko Hyomi, James Eickmann, and Charles M. Falco
Optical Sciences Center and Arizona Research Laboratories, University of Arizona, Tucson, Arizona 85721
(Received 17 March 1999)

We observe a systematic increase in interface perpendicular magnetic anisotropy (PMA) with increasing Au-interlayer thickness t_{Au} ranging from 1 to 5 ML in Cu/Co/Au/Cu(111), where misfit strain in Co due to the epitaxial growth increases with increasing t_{Au}. In addition, we have found an unexpected suppression of this variation of interface PMA with the use of Au overlayers instead of Cu. Also, the volume PMA significantly increases with the Au overlayer. [S0163-1829(99)04646-9]

I. INTRODUCTION

Surface and interface magnetic anisotropy has remained one of the most important subjects in modern magnetism. This anisotropy is largely a function of the quality and perfection of the surface or interface, and recent progress in deposition technology has allowed us to investigate such anisotropy in ultrathin films with samples controlled on the atomic scale.[1] The presence of Néel-type surface anisotropy based on the crystal symmetry and the magneto-elastic effect have been extensively discussed in many types of magnetic films and superlattices stacked with nonmagnetic layers. The uniaxial perpendicular magnetic anisotropy (PMA) is especially important, because of its large strength and the potential for storage applications in addition to its basic symmetry.

In Co/Pd superlattices, the interface PMA was found to be independent of the crystal orientation of the Co.[2] The interface PMA in Co/Au films also has been studied extensively.[3,4] When Co is epitaxially grown on Au a large strain develops due to the lattice mismatch of 14% between Co and Au, as well as the sharp interface due to the insolubility of Co into Au. Hence a magneto-elastic origin has been proposed to explain the large PMA of Co/Au superlattices.[5] The effect of strain on the interface PMA also has been discussed from the Co-thickness dependence of the PMA in comparison with other stacking systems such as Co/Ag and Co/Cu.[6–8] The strain dependence of the interface anisotropy is key to distinguishing between possible physical origins, such as structural and electronic effects. However, a systematic study of these materials while solely changing the strain has not been previously presented.

Our experimental results show that the in-plane lattice constant of Au on a Cu-buffer layer increases with increasing Au thickness, and that a subsequent Co layer can be epitaxially grown on that Au surface. Therefore, the Co/Au/Cu stacking system offers a good opportunity to systematically investigate the effect of strain on the interface PMA. In this paper, we report the results on single-crystal Co/Au/Cu(111) films prepared *simultaneously* with varying Au-interlayer thickness t_{Au} and Co thickness t_{Co}. This has allowed us to examine the effect of strain on the interface PMA under identical preparation conditions. We evaluate the interface anisotropy from the t_{Co} dependence of the PMA, which we determine by means of a spin-wave Brillouin technique taking into account a dipole field depending on t_{Co}. In addition, two types of overlayers consisting of Cu and Au are compared to examine the effect of overlayer material.

II. EXPERIMENT

We deposited films by molecular beam epitaxy, with a base pressure of 1×10^{-10} Torr. HF-cleaned Si(111) wafers were used as a substrate and annealed at 750 °C to show a 7×7-reconstructed surface. After cooling to room temperature, we deposited a 4.00 nm-thick Cu-buffer layer and varied t_{Au} from 0 to 5 ML using a step-movable shutter. After the Au-stepped wedge, the substrate was rotated by 90° and a Co-stepped wedge varying in thickness from 4 to 10 ML was deposited in the same manner to provide a matrix of samples of different t_{Au} and t_{Co}. For one set of samples, a Cu overlayer of 3.00 nm was deposited. Finally, a 3.50 nm-thick Au layer was deposited to prevent oxidation for both samples with and without the Cu overlayer. The Au-protective layer for the Cu overlayer was necessary, since we

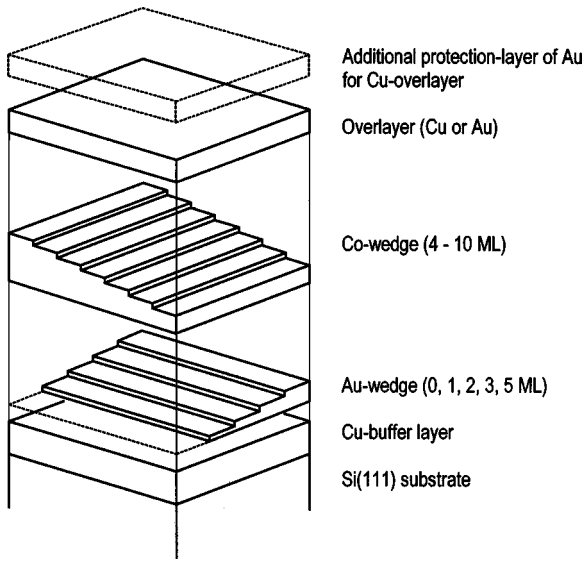

FIG. 1. Matrix sample geometry for the Au-overlayer/(Cu-overlayer)/Co stepped-wedge (4–10 ML)/Au stepped-wedge (0–5 ML)/Cu buffer-layer/Si(111) system.

observed oxide formation on a bare Cu surface. Geometry for our matrix sample is shown in Fig. 1. The deposition rates of the Au and Co both were 0.01 nm/sec, which were calibrated with an absolute accuracy of ±10% using Rutherford backscattering spectroscopy (RBS). RBS also confirmed the thickness distribution was within ±2% for one of the wedge samples. We used *in situ* reflected high energy electron diffraction (RHEED) and Auger electron spectroscopy (AES) for the evaluation of the film structure and quality. Magnetic properties were evaluated by *ex situ* spin-wave Brillouin scattering, the details of which were described elsewhere.[9] Saturation magnetization M_s was measured by a vibrating sample magnetometer (VSM).

III. RESULTS AND DISCUSSION

RHEED observations show narrow and sharp streak patterns indicating that the fcc-(111) structure with high crystallinity and flat surfaces are epitaxially grown through each of the layers. Continual RHEED observations for fcc-$[1\bar{1}0]$ of Cu and Au, or hcp-$[11\bar{2}0]$ of Co were performed using other planar samples, where the stacking of hcp-(0002) planes were identified in Co deposited on the Au interlayer rather than fcc-(111) planes by a cross-sectional high-resolution TEM. The skin-depth of the *e*-beam used for RHEED was estimated to be less than several Å with incidence angle of 0.5° and acceleration voltage of 15 kV. We observe the formation of Cu-silicide at the Cu/Si interface and a rotation of 30° around the [111] axis between the Si substrate and Cu-buffer layer.[10] Quantitative analysis of the RHEED patterns shows that the average in-plane lattice constant of Au on the Cu-buffer layer increases monotonically with increasing t_{Au} up to 5 ML at which point it has attained its bulk value. We find the in-plane lattice constant of the Co layer also is expanded by the Au interlayer up to 5 ML and then saturates. Figure 2 shows the in-plane strain in Co as a function of t_{Co}, which is derived from digitized RHEED images captured during the film growth. As can be seen, the strain in the Co layer is maximum at the Co/Au interface and gradually relaxes with increasing t_{Co}, which can be expressed by the $1/t_{\mathrm{Co}}$ law and understood as the relaxation of misfit strain.[11] On the other hand, the narrow streak patterns for Co indicate the good crystallinity of the Co layers. From the line width of the streak, the in-plane correlation length is estimated as a few nm. However, we could not observe a clear oscillation of the specular beam intensity of the RHEED as a function of Co thickness during the growth of Co films. Such a lack of RHEED oscillations was previously reported in Co/Cu(111), while they were observed in Co/Cu(100) prepared under identical conditions.[12] In addition, in epitaxial Co/Au superlattices, detailed x-ray diffraction showed an interface roughness of 1.5 ML.[4] Therefore, we conclude that the surface of Co (0002) is not sufficiently perfect to detect RHEED oscillations and it is an intrinsic structural property of this plane. However, we would note that we prepared matrix samples with systematically different misfit strain under identical preparation conditions and then we discussed the strain dependence of the anisotropy. AES analysis revealed no contamination of the Co layer within the sensitivity of 3%.

Figure 3 shows the spin-wave frequency as a function of

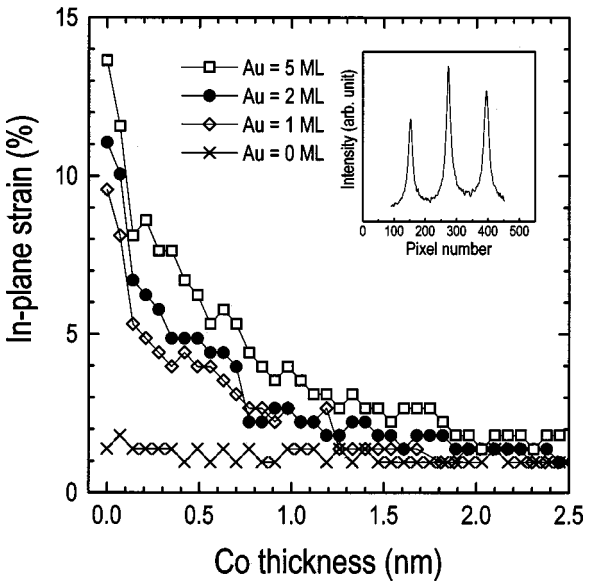

FIG. 2. In-plane strain of Co grown on Au/Cu(111) as a function of Co thickness with various thicknesses of Au interlayers. These data were obtained from intensity line scans of RHEED images as shown in the inset, with the lattice constant calibrated by the lattice spacing of the Si(7×7) substrate surface. RHEED images were continually captured in planar samples. The direction of the *e* beam was closely parallel to the $[1\bar{1}0]$ axis of Cu(111) plane. The bulk lattice constants are $a_{\text{fcc-Cu}}=0.2556$ nm, $a_{\text{fcc-Au}}=0.2884$ nm, and $a_{\text{hcp-Co}}=0.2507$ nm, respectively. The data points at Co thickness=0 nm correspond to the surface of a Cu-buffer layer or Au interlayers just before the Co layer starts to grow. It notes that clear oscillations of the specular beam intensity could not be observed (see text).

magnetic field in 5- and 10-ML-thick Co films. We have included effects of both the dipole and exchange fields in the calculation of spin-wave frequency, which are caused by a fluctuation of the magnetization due to the surface spin-wave observed by this light scattering method. The dipole correction is important since it is largely a function of t_{Co}. For this purpose, we modify the spin-wave theory by Cochran *et al.*[13] to be applicable for a magnetic film having out-of-plane magnetization due to a uniaxial PMA. We describe briefly the procedure for the calculation. A magnetic thin film with the thickness d lies in xz plane. The external field H is applied along the x axis and ϕ is the angle of the magnetization M with respect to the x axis. θ is the angle of the magnetization with respect to the z axis. ξ and η are small angles of deviation of the magnetization from its equilibrium position. ζ is the equilibrium direction of the magnetization vector. The equations of motion for the small deviation of the magnetization can be expressed, as follows:

$$M\dot{\eta}=-\gamma\partial E/\partial\xi+T_{\eta}, \tag{1}$$

$$M\dot{\xi}=\gamma\partial E/\partial\eta+T_{\xi}, \tag{2}$$

where T_{η} and T_{ξ} are the torque per unit area generated by the field due to the small deviation of the magnetization and $\gamma=g|e|/2mc$. We apply Cochran's procedure to our system and obtain expressions for the torque, as follows:

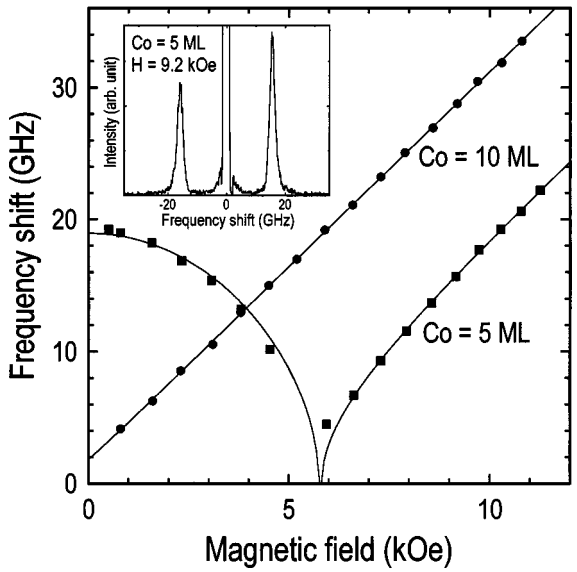

FIG. 3. Magnetic field dependence of the spin-wave Brillouin frequency in Co films sandwiched between a 3 ML Au-interlayer and an Au-overlayer. The inset shows the Brillouin spectrum from 5 ML of Co, where the transition between in-plane and out-of-plane magnetization appears at a critical field of 5.8 kOe. Below this field, the magnetization inclines from the film plane due to the perpendicular anisotropy. Solid lines are best-fitted calculations. Nonzero behavior of the spin-wave frequency appears at zero field (10 ML) or at the critical field (5 ML), mainly due to the dipole contribution depending on the Co thickness.

$$T_\eta = 4\pi M^2 \cos^2\phi(1-qd/2)\,\eta\gamma, \tag{3}$$

$$T_\xi = -2\pi M^2 q\, d\xi\, \gamma. \tag{4}$$

q is the wave vector of the spin wave, which is parallel to the z axis. The free energy per unit of the system can be expanded for small ξ and η, as follows:

$$E = E_0 + (E_{\xi\xi}\xi^2 + 2E_{\xi\eta}\xi\eta + E_{\eta\eta}\eta^2)/2. \tag{5}$$

ξ and η are characterized by time and space variations as $e^{i\omega t}$ and e^{iqx}. Therefore,

$$(\omega/\gamma)^2 = (E_{\xi\xi}E_{\eta\eta} - E_{\xi\eta}^2)/M^2 + 2\pi qd(E_{\eta\eta} - E_{\xi\xi}\cos^2\phi) + O[(qd)^2]. \tag{6}$$

The equilibrium position of the magnetization is derived from angular differential of the free energy and thus $\theta = \pi/2$ in this system. With neglecting higher order $O(qd)^2$, we obtain,

$$(\omega/\gamma)^2 = (E_{\theta\theta}E_{\phi\phi} - E_{\theta\phi}^2)/M_s^2 + 2\pi qd(E_{\phi\phi} - E_{\theta\theta}\cos^2\phi). \tag{7}$$

The second term corresponds to the dipole contribution. The free energy per unit of the system can be expressed as $E = E_{\text{Zeeman}} + E_{\text{magnetostatic}} + E_{\text{anisotropy}}$. Within our experimental resolution of 0.2 GHz, in the Co/Au/Cu(111) plane the spin-wave frequency is independent of the angle between the in-plane crystal axis and the applied field. Thus the in-plane crystal anisotropy can be omitted from our calculation, in which the uniaxial anisotropy contribution is expressed in the free energy as follows, $E_{\text{anisotropy}} = -K_u^{(1)}\sin^2\phi - K_u^{(2)}\sin^4\phi$. A positive value of each anisotropy constant indicates perpendicular anisotropy. Therefore,

$$E = -HM_s\cos\phi + (2\pi M_s^2)\sin^2\phi - K_u^{(1)}\sin^2\phi - K_u^{(2)}\sin^4\phi. \tag{8}$$

The spin-wave frequency is finally calculated by torque equations of the precession of magnetization under effective fields taking account of the exchange field in addition to the dipole contribution. We are able to fit the measured field dependence of the spin-wave frequency in each sample using the above procedure.

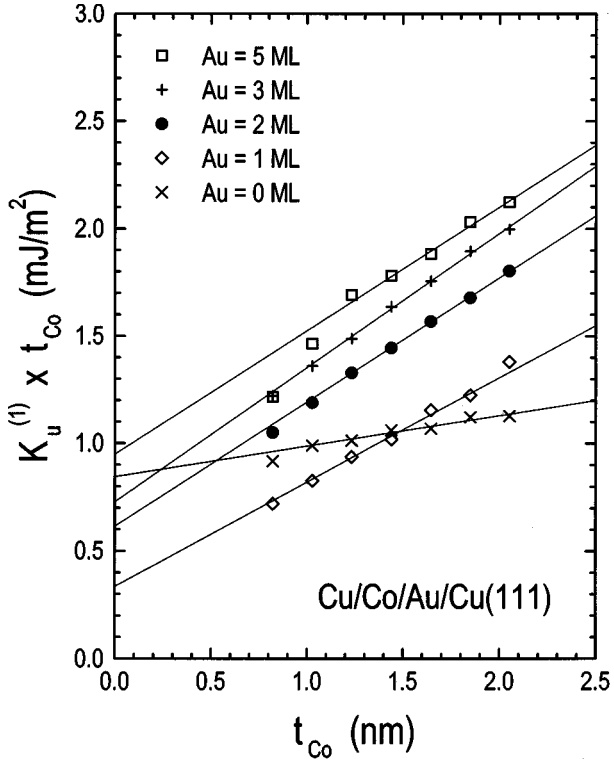

FIG. 4. Product of perpendicular anisotropy constant $K_u^{(1)}$ obtained from spin-wave measurements and t_{Co} as a function of t_{Co}, with various t_{Au} and with *Cu overlayers*. Solid lines are least square fits for $t_{\text{Co}} \geqq 1.0$ nm. Experimental errors are less than 0.04 mJ/m^2.

From the field dependence of spin-wave frequency, we derive the first- and second-order anisotropy constants $K_u^{(1)}$ and $K_u^{(2)}$. The results for $K_u^{(1)}$ for various t_{Au} in Cu/Co/Au/Cu(111) are shown in Fig. 4, where the product of $K_u^{(1)}t_{\text{Co}}$ is plotted as a function of t_{Co}. We observe a linear relation for each Au interlayer. This indicates the existence of an interface anisotropy that can be phenomenologically represented as $K_u^{(1)}t_{\text{Co}} = K_{u,I}^{(1)} + K_{u,V}^{(1)}t_{\text{Co}}$, where the first term is the sum of the interface anisotropy and the $K_{u,V}$ term is the volume anisotropy.[1] From this linearity we can determine the value of interface anisotropy from the intercept on the vertical axis. A slight deviation from linearity for $t_{\text{Co}} \leqq 1$ nm is commonly observed in Co/Au superlattices, and effects of strain and misfit dislocation have been discussed by others.[3,5,7] As can be seen in Fig. 4, we find a systematic variation of the interface PMA with t_{Au}. Above 1 ML of Au, the interface PMA monotonically increases with increasing t_{Au}, which coincides with the monotonic increase in the in-plane strain of Co. The

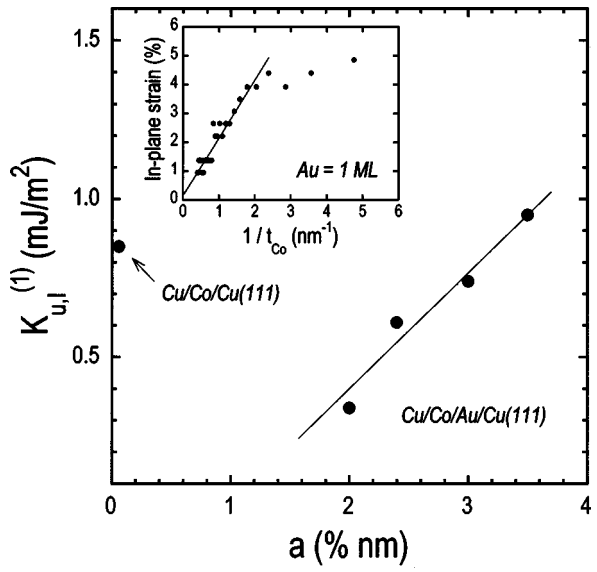

FIG. 5. Interface perpendicular anisotropy constant $K_{u,I}^{(1)}$ as a function of strain parameter a, which is determined from the $1/t_{\mathrm{Co}}$ dependence of in-plane strain (the inset and see text). With Au interlayers, the good proportionality of the interface anisotropy to the strain is observed.

effect of misfit strain on the anisotropy has been discussed previously based on a critical layer thickness t_c between coherent and incoherent film growth in the epitaxial system, as follows:[6,14]

$$K_I = K_N + K_\lambda ,$$

$$K_V = K_{\mathrm{MC}} \quad \text{for } t_{\mathrm{Co}} > t_c , \tag{9}$$

$$K_I = K_N ,$$

$$K_V = K_{\mathrm{MC}} + K_{\mathrm{ME}} \quad \text{for } t_{\mathrm{Co}} < t_c . \tag{10}$$

Above t_c, the magneto-elastic contribution K_λ is included in the interface anisotropy, where K_N is the Néel-type surface anisotropy. The volume anisotropy K_V without the shape anisotropy $-2\pi M_s^2$ is shown as a magneto-crystalline anisotropy K_{MC}. Below t_c, the magneto-elastic anisotropy K_{ME} is added to K_V. Since t_c is nearly equal to 0 ML, as shown in Fig. 2, Eq. (9) for the K_I is applicable. This agrees with our experimental result, where the interface PMA increases with increasing misfit strain. Therefore, we conclude that the interface PMA depends on the interface strain in this Cu/Co/Au/Cu(111) system. The relation between the in-plane misfit strain ϵ and the interface anisotropy constant $K_{u,I}^{(1)}$ is shown in Fig. 5. As shown in the inset, the strain is well expressed by the equation,

$$\epsilon = (a/t_{\mathrm{Co}}) + b, \tag{11}$$

except for the initial few ML's of Co. The constant a indicates the amplitude of thickness dependence of the misfit strain near the lower Co/Au interface, and b is the thickness-independent strain. Therefore, the former a can contribute to the interface anisotropy through the magnetoelastic effect as

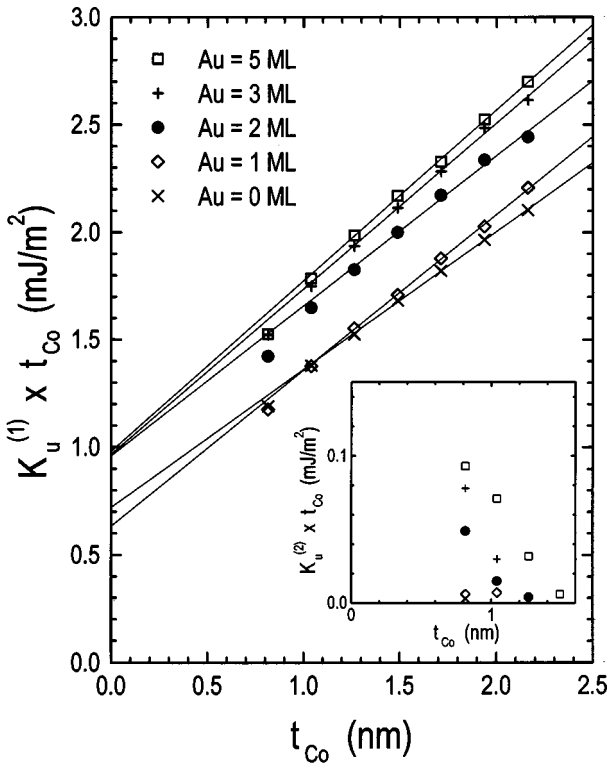

FIG. 6. Plot of $K_u^{(1)} t_{\mathrm{Co}}$ vs t_{Co} with various t_{Au} and with an *Au overlayer*. The inset shows the higher anisotropy contribution $K_u^{(2)} t_{\mathrm{Co}}$ as a function of t_{Co}.

discussed above. In fact, it is clearly shown that ϵ increases monotonically with increasing a in our Cu/Co/Au/Cu(111) system. It should be noted that the value of b is less than 0.2% for this system and thus is negligible, while that is 1.1% for the Cu/Co/Cu(111) system. On the other hand, K_V shows a constant value for values of $t_{\mathrm{Au}} \geqq 1$ ML. This indicates the crystallinity of Co is stable for $t_{\mathrm{Au}} \geqq 1$ ML and also the interface-induced misfit strain does not significantly affect the K_V in those Co films thicker than several ML's discussed here.

The interface PMA, $K_I = 0.85\ \mathrm{mJ/m^2}$ in Co directly grown on Cu is markedly higher than $K_I = 0.34$–$0.72\ \mathrm{mJ/m^2}$ of Co deposited on thin Au interlayers, although the strain in the former is much smaller than that in the latter. Actually, the in-plane lattice constant in Cu/Co/Cu is constant in the range of $t_{\mathrm{Co}} \leqq 2.5$ nm that we examined, and thus the growth mode is coherent. Therefore, we conclude the intrinsic $K_N = 0.43\ \mathrm{mJ/m^2}$ at the Co/Cu interface is higher than that at the Co/Au interface. Also, we demonstrate that the $K_V = 0.14\ \mathrm{MJ/m^3}$ in Cu/Co/Cu is abruptly transformed into $K_V = 0.49\ \mathrm{MJ/m^3}$ in Cu/Co/Au with only one ML of Au interlayer. It should be noted that the value of K_V in Cu/Co/Au is in the range 0.5–$0.6\ \mathrm{MJ/m^3}$, which is comparable with the value of $0.56\ \mathrm{MJ/m^3}$ recently determined in well-characterized hcp-Co.[15] The meaningfully smaller value of K_V in Cu/Co/Cu is possibly due to the fcc phase and slight contamination of other planes like (100) and (110).[16,17]

Next, we show the dramatic effects of an overlayer on the PMA. As shown in Fig. 6, with the use of an Au overlayer instead of Cu, we find that the variety of interface PMA values observed with the Cu overlayer is strongly suppressed. The upper limit of $K_I = 0.96\ \mathrm{mJ/m^2}$ at $t_{\mathrm{Au}} = 5$ ML is

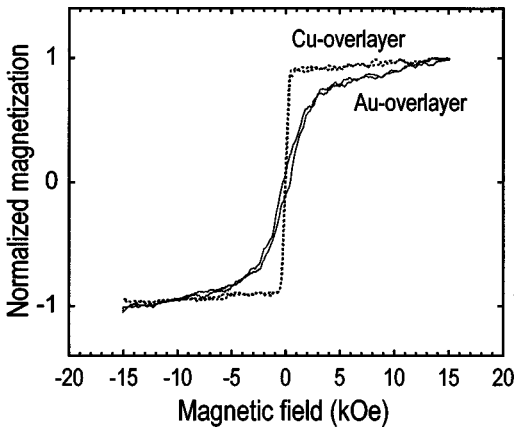

FIG. 7. Magnetization curves measured using a VSM, for 5 ML of Co with 1 ML of the Au interlayer with the Cu (a dotted line) or Au overlayer (a solid line). The external field is applied along with the film plane.

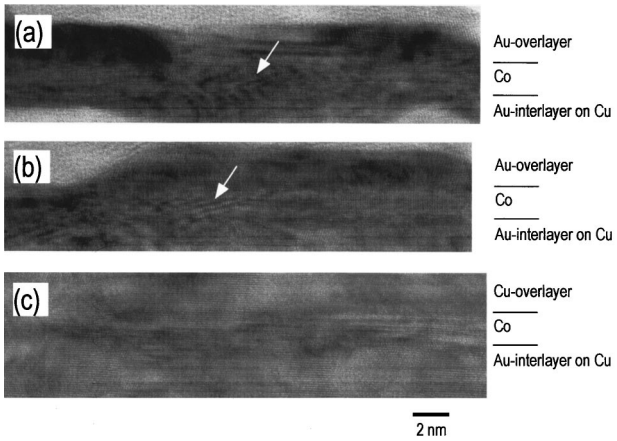

FIG. 8. Cross-sectional TEM images for 10 ML of Co with the Au-overlayer (a),(b), in comparison with that with the Cu-overlayer (c). For the Au overlayer, local and inhomogeneous Moiré fringes can be seen (indicated by an arrow and see text).

not changed by the Au overlayer, although the interface anisotropy with thinner Au interlayers significantly increases by a factor of 1.4–2. Also, the interface anisotropy of Co directly deposited on Cu decreases to $K_I = 0.72\,\mathrm{mJ/m^2}$ with the Au overlayer. Simply adding or subtracting a constant value of K_N difference between the Au and Cu overlayers, $K_N^{(\mathrm{Co/Au})} - K_N^{(\mathrm{Co/Cu})}$, cannot explain this suppression of the t_{Au} dependence of interface anisotropy with the Au overlayer. It should be noted that the upper limit of $K_I = 1.1\,\mathrm{mJ/m^2}$ including the $K_u^{(2)}$ contribution is comparable with the value of interface anisotropy reported in Co/Au superlattices.[1,7] This significant change in the perpendicular anisotropy due to the Au overlayer is also confirmed by means of a magnetization curve using a VSM. Figure 7 shows a typical example for 5 ML of Co with 1 ML of the Au interlayer with Cu or Au overlayer, in which the external field is applied along with the film plane. Here, the product of the total anisotropy K_u^{Total} including the in-plane shape anisotropy and the Co thickness is determined by the spin-wave Brillouin as $K_u^{\mathrm{Total}} t_{\mathrm{Co}} = -0.49\,\mathrm{mJ/m^2}$ (in-plane magnetization without external field) for the Cu overlayer, and $K_u^{\mathrm{Total}} t_{\mathrm{Co}} = 0.06\,\mathrm{mJ/m^2}$ (perpendicular magnetization without external field) for the Au overlayer, respectively. Therefore, a significant change in the magnetization curve for the in-plane direction can be seen, as shown in Fig. 7. The easy axis for the magnetization is in-plane for the Cu overlayer. On the other hand, the magnetization curve for the Au overlayer indicates the hard axis for the magnetization, since a Polar-Kerr measurement with applying the field normal to the film plane shows a square hysteresis curve. This result shows a good agreement with the observation using the Brillouin for the significant change in the perpendicular anisotropy due to the Au overlayer. A possible explanation for this change in the variation of interface anisotropy is the additional formation of dislocation and thickness-dependent strain in Co due to the Au coverage. We observe Moiré fringes in a Co layer with Au overlayer using a high-resolution cross-sectional TEM (JEOL JEM2010), as shown in Fig. 8. These fringes can be caused by structural domains with different lattice constants and with formation of dislocations. The fringes are local and the spacings of the fringes are not uniform. However, the typical value of the spacing is in the range 0.8–1.6 nm, which corresponds to local strain of 12–20 %, if the fringes are made of a strained and a non-strained domain. This observation supports the presence of a deformation of the lattice structure and the additional strain in Co after capping with an Au overlayer. Previously RHEED analysis showed that Au growth on Co was incoherent and stress free for coverages greater than 1 ML.[18] Therefore, the magnetoelastic effect due to the Au overlayer on the interface PMA was not taken into consideration.[7,8] Our finding is that the additional strain and misfit dislocation of Co caused by the Au overlayer is rather inhomogeneous and the relaxation of the strain occurs locally, even though good epitaxial growth can be continually observed in the Au overlayer by means of RHEED. This feature of the additional strain and its relaxation is apparently different from the misfit strain of Co grown on the underlayer with larger lattice constant. In addition, the magnitude of the volume anisotropy significantly increases, e.g., from $K_V = 0.57\,\mathrm{MJ/m^3}$ to $0.78\,\mathrm{MJ/m^3}$ for $t_{\mathrm{Au}} = 5$ ML. If we assume that the Au overlayer induces dislocation-free and thus thickness-independent strain inside Co in addition to the dislocation formation around the interface, Eq. (10) shows it is reasonable to apply this framework of strain-modified volume anisotropy to our experimental result. Our experimental results in single ultrathin films may be general in superlattice samples. The strain dependence of the interface PMA and the effects of overlayer-induced local strain can be observed, if we separate the effect of uniform strain throughout the superlattice structure.

Finally, we comment on the behavior of the higher order PMA, $K_u^{(2)}$. From our fitting of the field dependence of the spin-wave frequency, the contribution of $K_u^{(2)}$ appears in thin Co films. The value of $K_u^{(2)}$ is relatively small, ranging from 1 to 9% of $K_u^{(1)}$. However, we find that $K_u^{(2)}$ increases with decreasing t_{Co} and shows the interface contribution. We also observe a systematic increase in the $K_u^{(2)}$ with increasing t_{Au}, even with the Au overlayer, as shown in the inset of Fig. 6.

IV. SUMMARY

In this paper, we prepared simultaneously epitaxially grown Co/Au/Cu(111) films with varying t_{Co} and t_{Au}. From

the field dependence of the spin-wave Brillouin frequency, we found a strain-induced increase in the interface perpendicular anisotropy in Cu/Co/Au/Cu(111). Moreover, we found that such variations of the interface anisotropy are strongly suppressed by the use of an Au overlayer instead of Cu. At the same time, we observe an increase in the volume anisotropy. These unexpected effects of the Au overlayer motivate the investigation of the form of strain in epitaxial films *after forming* overlayer, and related magnetic phenomena in metallic ultrathin films with large mismatch of the lattice constants.

ACKNOWLEDGMENTS

The authors are indebted to S. Kondoh of ASAHI Glass Co. Ltd. for his TEM observation, and M. Imakawa and T. Hiruma of ASAHI-KOMAG Co. Ltd. for their VSM measurement. This research was partially supported by U.S. DOE Grant No. DE-FG02-93ER45488.

*Permanent address: ASAHI-KOMAG Co., Yonezawa, 992-11, Japan.

[1] See various articles in *Ultrathin Magnetic Structure I & II*, edited by B. Heinrich and J. A. C. Bland (Springer-Verlag, Berlin, 1994).

[2] B. N. Engel, C. D. England, R. A. Van Leeuwen, M. H. Wiedmann, and C. M. Falco, Phys. Rev. Lett. **67**, 1910 (1991).

[3] F. J. A. den Broeder, D. Kuiper, A. P. van der Mosselaer, and W. Hoving, Phys. Rev. Lett. **60**, 2769 (1988).

[4] C. H. Lee, Hui He, F. Lamelas, W. Vavra, C. Uher, and Roy Clarke, Phys. Rev. Lett. **62**, 653 (1989).

[5] C. H. Lee, Hui He, F. J. Lamelas, W. Vavra, C. Uher, and Roy Clarke, Phys. Rev. B **42**, 1066 (1990).

[6] C. Chappert and P. Bruno, J. Appl. Phys. **64**, 5736 (1988).

[7] T. Kingetsu and K. Sakai, Phys. Rev. B **48**, 4140 (1993).

[8] J. Kohlhepp, H. J. Elmers, and U. Gradmann, J. Magn. Magn. Mater. **121**, 487 (1993).

[9] A. Murayama, K. Hyomi, J. Eickmann, and C. M. Falco, J. Appl. Phys. **82**, 6186 (1997).

[10] C. S. Liu, S. R. Chen, W. J. Chen, and L. J. Chen, Mater. Chem. Phys. **36**, 170 (1993).

[11] C. Chappert, P. Beauvillain, P. Bruno, J. P. Chauyineau, M. Galtier, K. Le Dang, C. Marlière, R. Mégy, D. Renard, J. R. Renard, J. Seiden, F. Trigui, P. Veillet, and E. Vélu, J. Magn. Magn. Mater. **93**, 319 (1991).

[12] F. Huang, M. T. Kief, G. J. Mankey, and R. F. Willis, Phys. Rev. B **49**, 3962 (1994).

[13] J. F. Cochran, J. Rudd, W. B. Muir, B. Heinrich, and Z. Celinski, Phys. Rev. B **42**, 508 (1990).

[14] R. Jungblut, M. T. Johnson, J. aan de Stegge, A. Reinders, and F. J. A. den Broeder, J. Appl. Phys. **75**, 6424 (1994).

[15] M. Farle, Y. Henry, and K. Ounadjela, Phys. Rev. B **53**, 11 562 (1996).

[16] A. Murayama, K. Hyomi, J. Eickmann, and C. M. Falco, J. Appl. Phys. **83**, 613 (1998).

[17] B. N. Engel, C. D. England, A. Van Leeuwen, M. H. Wiedmann, and C. M. Falco, J. Appl. Phys. **70**, 5873 (1991).

[18] B. N. Engel, M. H. Wiedmann, and C. M. Falco, J. Appl. Phys. **75**, 6401 (1994).